

**LA-8735-PR**

Progress Report

C.3

CIC-14 REPORT COLLECTION

**REPRODUCTION  
COPY**

**Space Nuclear Safety and Fuels Program**

**November 1980**

University of California



**LOS ALAMOS SCIENTIFIC LABORATORY**

Post Office Box 1663 Los Alamos, New Mexico 87545

The four most recent reports in this series, unclassified, are LA-8582-PR, LA-8713-PR, LA-8714-PR, and LA-8715-PR.

This report was not edited by the Technical Information staff.

This work was supported by the US Department of Energy, Division of Space and Terrestrial Systems.

**DISCLAIMER**

This report was prepared as an account of work sponsored by an agency of the United States Government. Neither the United States Government nor any agency thereof, nor any of their employees, makes any warranty, express or implied, or assumes any legal liability or responsibility for the accuracy, completeness, or usefulness of any information, apparatus, product, or process disclosed, or represents that its use would not infringe privately owned rights. Reference herein to any specific commercial product, process, or service by trade name, trademark, manufacturer, or otherwise, does not necessarily constitute or imply its endorsement, recommendation, or favoring by the United States Government or any agency thereof. The views and opinions of authors expressed herein do not necessarily state or reflect those of the United States Government or any agency thereof.

LA-8735-PR  
Progress Report

UC-23  
Issued: February 1981

# Space Nuclear Safety and Fuels Program

## November 1980

Compiled by  
S. E. Bronisz



## ABSTRACT

This formal monthly report covers the studies related to the use of  $^{238}\text{PuO}_2$  in radioisotopic power systems carried out for the Space and Terrestrial Systems Division of the U. S. Department of Energy by the Los Alamos National Laboratory.

Most of the studies discussed here are of a continuing nature. Results and conclusions described may change as the work continues. Published reference to the results cited in this report should not be made without the explicit permission of the person in charge of the work.

---

## SPACE NUCLEAR SAFETY AND FUELS PROGRAM

NOVEMBER 1980

Compiled by  
S. E. Bronisz

### I. GENERAL-PURPOSE HEAT SOURCE

#### A. Impact Tests (F. W. Schonfeld)

The postmortem examinations of the four fueled clads impacted in the Design Verification Test (DVT) series were extended this month. Details of the DVT impacts were presented in the August, September, and October monthly reports. Briefly, four General-Purpose Heat Source (GPHS) modules of the LMRF design (CBCF insulation and end loading of the graphite impact shell (GIS)) were impacted at 820°C or 850°C at 58 mps at three orientations 0° (end-on), 27°, and 90° (2 tests). The 0° and 27° tests resulted in deformation of the fueled iridium capsules, while both 90° tests resulted in severe, non-ductile cracking of the capsules. The observed cracking in the 90° orientation was due to the design-specific stress state resulting from the effective void in the CBCF insulation volume.

1. Fuel analyses. The particle size distributions of the four fuel pellets are given in Table I. The size range for IRG-88 is truncated because the fuel was not recovered quantitatively.

The spectrochemical analyses of three of the fuel pellets are listed in Table II. The small differences among the elemental contents have no obvious relationship to the impact responses.

Typical microstructures of the four fuel pellets are illustrated by the photomicrographs shown in Fig. 1. Again, there are no extraordinary variations in the fuel that might explain the failure of IRG-88 and the near failure of IRG-90. Analysis of the graphite components from IRG-88 revealed that 3.5 mg of fuel had been released from the clad and trapped by the graphite.

2. Iridium analyses. The spectrochemical analyses of samples of three of the iridium clads are listed in Table III. Samples from each cup of the three capsules in Table III were examined by Auger Electron spectroscopy. Thorium, carbon, and oxygen were detected in concentrations and distributions normal for the DOP-26 iridium alloy.

The analyses of the iridium provide no better reasons for the cracks observed in IRG-88 and IRG-90 than do the fuel analyses. It seems quite likely that the responses of IRG-88 and IRG-90 were related to the specific stress state that exists in the 90° orientation and not to any mechanical or chemical difference among the components of the DVT modules. The main factor to be explored is the importance of the following impact assembly to the deformation of the fueled clads in the leading impact assembly. The cracks in IRG-90 occurred with very little prior strain, suggesting that the impact of the GPHS-LMRF module on its broad face might result in clad failures. This is

important, because the broad-face orientation is believed to be the most likely and it puts all four fueled clads at risk.

#### B. Fine-Weave Pierced Fabric Shear Tests (R. Zocher, M. Stout)

The position of a GPHS module in the heat-source stack is maintained by two lock members, which are placed in recesses in the broad face of the aeroshell. The lock members are made of fine-weave pierced fabric (FWPF) graphite, as is the aeroshell, and are visible on the top of the module stack shown in Fig. 2. The FWPF graphite is known to have anisotropic properties, so we conducted a series of shear tests to obtain data on the effects of that anisotropy in the shearing response of the lock member.

A precision fixture, shown in Fig. 3 as an exploded drawing and in the photograph in Fig. 4, was designed so that two lock members could be tested simultaneously.

The microstructures of the equatorial planes of the four orientations tested are shown schematically in Fig. 5. Five tests of two lock members each were run at each of the orientations depicted in the figure. In each orientation the five tests replicated one another quite closely.

The stress-deflection curve for each of the orientations is shown in Fig. 6. The rotation of the X-Y plane about the Z-axis when the shearing direction is perpendicular to the Z-axis had a small effect. The samples with X and Y directions at  $45^\circ$  were somewhat softer than when those directions were at  $0^\circ$  and  $90^\circ$ , but the general shapes of the curves were similar.

The orientation of the Z-axis bundles when they were in the plane of shear had quite a strong effect on the shape of the stress-deflection curves, as seen in Figs. 6c and 6d. When the Z-bundles were parallel to the shearing direction, the sample was stiffer and its deflection curve was monotonic to the ultimate stress, whereas in the samples with the Z-bundles perpendicular to the shear direction the stress-deflection curve exhibited a pseudo-yield point, but had a higher ultimate strength.

These shear tests are summarized in Table IV. The orientation of the locking member about its axis will be random in use, because of the rotational freedom. If the FWPF is oriented so that its Z-bundles are parallel to the axis of the lock member, the rotational orientation will have much less of an effect on the shearing properties than if the Z-bundles are perpendicular to the lock member axis. Similarly, the parallel orientation displays stiffness and early strength, whereas the perpendicular orientation results in higher, but later, strength. The selection of one orientation over the other would depend on the amount of deflection that can be tolerated in the heat source stack and the actual strength requirements.

#### C. Fuel Development (R. Kent)

Los Alamos fuel pellet GP-19 was encapsulated in iridium to form GPHS fueled clad IRG-62, which will be used in the reentry simulation next month. A total of 37 Los Alamos-fabricated fuel pellets has been encapsulated.

The dimensions of seven Savannah River Laboratory (SRL) pellets received by Los Alamos for encapsulation and testing are given in Table V. Each of the SRL pellets had surface cracks like those visible in Fig. 7.

Los Alamos employees R. Behrens and G. Melton visited the Savannah River Plant (SRP) to assist in the GPHS production startup.

## II. SYSTEMS SUPPORT

### A. Stirling Isotope Power System (D. Pavone)

The accumulated exposure time of the 800<sup>0</sup> test assembly was 25,678 h on December 1, 1980.

### B. Multi-hundred Watt (D. Pavone, C. Frantz)

The Multi-hundred Watt fuel sphere assembly (FSA) MHFT-68 was tested in a simulation of the minimum-gamma reentry and impact of the Galileo heat source. The sample was aged for 110 h at a surface temperature of 1210<sup>0</sup>C, subjected to a reentry heat pulse with a maximum iridium temperature of 1792<sup>0</sup>C and impacted at 81.7 mps and 1579<sup>0</sup>C. Radiographs taken after aging showed that the fuel sphere was broken and that the pieces were separated.

The impact of the sample occurred with the GIS cap oriented at 180<sup>0</sup> to the initial impact point. The shell was delaminated, but the body was not split.

Photographs of the impacted sample with the graphite removed are shown in Fig. 8. The iridium shell was oriented with its weld plane nearly parallel to the target. No hoop fractures or tensile tears on the back side of the iridium were observed, nor were fingerprint cracks or fuel-fragment punch displacements seen on the impact face. A gray, metallic deposit was observed adhering to the iridium exterior on the decontamination-cover weld bead. On exposure to air this deposit oxidized to a yellowish-white material, which was identified by X-ray diffraction analysis as MoO<sub>3</sub>. The source of the molybdenum deposit is unknown.

The average diameter of the impacted sample was 43.66 mm, equivalent to a diametral strain of +7.4%, and the height of the impacted shell was 30.07 mm, indicating a height strain of -26.0%.

Analysis of the recovered graphite debris revealed a total plutonium content of 47 µg and a phosphorous content equivalent to 82 ppm.

Metallographic examination of the microstructure of the iridium indicated that the weld microstructure was excellent, as shown in Fig. 9. The grain size of one of the hemispheres of the iridium was nonuniform, varying from 5-12 grains across the thickness, with the average being 8.8 grains/thickness. The microstructures shown in Fig. 10 illustrate the variation of grain size observed for this hemisphere. The average grain size of the other hemisphere was 10.1 grains/thickness.

The appearance of flat grains of iridium on the interior surface of the iridium shell was noted, as was a slight amount of iridium transport. These features are illustrated in Figs. 11 and 12.

Metallographic examination of samples of the plutonia sphere showed that material near the impact face was denser than that away from the surface region, however, there was no evidence of deformation of individual grains that would suggest plastic deformation of the plutonia. Figure 13 shows microstructures of the plutonia sphere.

Chemical analysis of a sample of the plutonia sphere indicated a phosphorous content of 20 ppm. Spectrographic analysis indicated the following elements to be present at levels exceeding the detection limits.

|              |              |
|--------------|--------------|
| Si - 310 ppm | Fe - 150 ppm |
| Zn - 25 ppm  | Cr - 25 ppm  |
| Ta - 500 ppm | Ni - 9 ppm   |
| Ca - 7 ppm   | Ti - 15 ppm  |
| Al - 25 ppm  | Mo - 15 ppm  |
| Mg - 300 ppm |              |

### III. LIGHT-WEIGHT RADIOISOTOPIC HEATER UNIT (R. Kent, R. Tate)

#### A. Specifications and Analyses

The Specification Document, CMB-11-RDH-80-105, "The Specification for Fabrication and Encapsulation of LWRHU Pellets and Assembly of Heater Units," has been written and submitted to DOE/STS for approval.

To date, we have hot pressed 7 lots of 16-each LWRHU pellets (112 pellets). Each lot was fabricated, using constant fabrication parameters, from the same lot of SRP feed material, nominally enriched at 83.5 at.% Pu-238. The fabrication parameters and sintered dimensions for these pellet lots are summarized in Table VI. Two pellets from each lot were sampled for analyses. Spectrochemical data for the 7 pellet lots are summarized in Table VII. Isotopic chemical data for 5 of these lots are listed in Table VIII. The isotopic data, combined with the weight data from Table VI, yielded a calculated thermal inventory of 1.11 watts per pellet on the delivery date, April 30, 1980. The specification is  $1.10 \pm 0.03$  watts.

No flight-quality hardware has been received. However, a number of pellets have been encapsulated for testing at Los Alamos. The specification for decontamination of the welded capsules is 220 cpm (swipe). All capsules welded to date have been decontaminated to zero swipe.

The specified neutron emission rate for these pellets is 6000 n/s-g  $^{238}\text{Pu}$ . Two of the test pellets have been counted and the average neutron emission rate measured was  $5200 \pm 50$  n/s-g  $^{238}\text{Pu}$ . Finally, the specified leak rate for welded capsules is  $1 \times 10^{-6}$  cm<sup>3</sup>/s helium. All capsules welded for testing have had leak rates less than  $1 \times 10^{-9}$  cm<sup>3</sup>/s helium.

#### B. Encapsulation

Four UO<sub>2</sub> simulant pellets were encapsulated in Pt-30 Rh hardware for testing.

All welding procedures have been written, tested, and approved. The 45 pellets for Hughes Aircraft will be encapsulated into the Pt-30 Rh flight-quality hardware when it is received at Los Alamos.

#### C. Safety

A presentation on the development of the LWRHU was made to the Interagency Nuclear Safety Review Panel at the meeting to review the Galileo and Solar/Polar Preliminary Safety Analysis Report held in Germantown, MD, on November 19, 1980.

TABLE I  
 FRACTIONAL DISTRIBUTION OF PARTICLE SIZES OF IMPACTED FUELS

| <u>Size<br/>(mm)</u> | <u>IRG-87<br/>SRGPHS - 25</u> | <u>IRG-88<br/>SRGPHS - 27</u> | <u>IRG-89<br/>SRGPHS - 28</u> | <u>IRG-90<br/>SRGPHS - 29</u> |
|----------------------|-------------------------------|-------------------------------|-------------------------------|-------------------------------|
| +6                   | 0.728                         | 0.490                         | 0.240                         | 0.529                         |
| -6, + 2              | 0.173                         | 0.281                         | 0.478                         | 0.334                         |
| -2, + 0.841          | 0.045                         | 0.134                         | 0.183                         | 0.097                         |
| -0.841, + 0.420      | 0.017                         | 0.050                         | 0.051                         | 0.023                         |
| -0.420, + 0.177      | 0.009                         | 0.045                         | 0.025                         | 0.009                         |
| -0.177, + 0.125      | 0.002                         | N.D.                          | 0.004                         | 0.001                         |
| -1.125, + 0.074      | 0.004                         | "                             | 0.005                         | 0.002                         |
| -0.074, + 0.044      | 0.005                         | "                             | 0.003                         | 0.001                         |
| -0.044, + 0.030      | 0.006                         | "                             | 0.002                         | 0.0009                        |
| -0.030, + 0.020      | 0.003                         | "                             | 0.001                         | 0.0005                        |
| -0.020, + 0.010      | 0.005                         | "                             | 0.003                         | 0.0012                        |
| -0.010               | 0.003                         | "                             | 0.004                         | 0.0013                        |

TABLE II  
SPECTROGRAPHIC ANALYSES OF  
IMPACTED FUELS

|    | <u>SRGPHS-25</u> | <u>SRGPHS - 27*</u> | <u>SRGPHS - 29</u> |
|----|------------------|---------------------|--------------------|
| Li | 1                | 1                   | 1                  |
| Be | <1               | <1                  | <1                 |
| B  | <1               | 5                   | 4                  |
| Na | 2                | 2                   | <2                 |
| Mg | 50               | 300                 | 50                 |
| Al | 140              | 35                  | 40                 |
| Si | 400              | 350                 | 550                |
| K  | <5               | <5                  | <5                 |
| Ca | >750             | 750                 | >750               |
| Ti | 15               | 10                  | 10                 |
| V  | <3               | <3                  | <3                 |
| Cr | 9                | 25                  | 20                 |
| Mn | 3                | 5                   | 2                  |
| Fe | 310              | 340                 | 270                |
| Co | <3               | 10                  | <3                 |
| Ni | 6                | 45                  | 30                 |
| Cu | <1               | <1                  | <1                 |
| Zn | 15               | 50                  | 15                 |
| Rb | <10              | <10                 | <10                |
| Sr | 10               | <5                  | <5                 |
| Y  | <25              | <25                 | <25                |
| Zr | <100             | <100                | <100               |
| Nb | <10              | <10                 | <10                |
| Mo | 5                | 10                  | 4                  |
| Ag | 50               | 40                  | 7                  |
| Cd | <10              | <10                 | <10                |
| Sn | <5               | <5                  | <5                 |
| Ba | 15               | <2                  | 2                  |
| La | <25              | <25                 | <25                |
| Hf | <25              | <25                 | <25                |
| Ta | 100              | 500                 | 400                |
| W  | <10              | <10                 | <10                |
| Re | <25              | <25                 | <25                |
| Pb | <5               | <5                  | <5                 |
| Bi | <1               | <1                  | <1                 |

\*Additionally, P was determined by a wet method to be 20 ppm.

TABLE III  
COMPOSITIONS OF IMPACTED  
Ir-0.3% W CAPSULES  
(SPECTRO. SURVEY)

|    | <u>IRG-88</u> | <u>IRG-89</u> | <u>IRG-90</u> |
|----|---------------|---------------|---------------|
| Li | <30           | <30           | <30           |
| Be | <3            | <3            | <3            |
| B  | <30           | <30           | <30           |
| Na | <300          | <100          | <100          |
| Mg | 5             | 15            | 15            |
| Al | 60            | 40            | 40            |
| Si | 10            | 30            | 30            |
| P  | <300          | <300          | <300          |
| K  | <1000         | <2000         | <2000         |
| Ca | <3            | 3             | 3             |
| Ti | <30           | <30           | <30           |
| V  | <30           | <30           | <30           |
| Cr | 30            | 20            | 10            |
| Mn | <10           | <10           | <10           |
| Fe | 40            | 20            | 20            |
| Co | <10           | <10           | <10           |
| Ni | 10            | <20           | <20           |
| Cu | 25            | 3             | 3             |
| Zn | <50           | <50           | <50           |
| Ga | <30           | <30           | <30           |
| Ge | <30           | <30           | <30           |
| Sr | <3            | <3            | <3            |
| Zr | <300          | <300          | <300          |
| Nb | <300          | <300          | <300          |
| Mo | <300          | <300          | <300          |
| Ru | <30           | <30           | <30           |
| Rh | <30           | <30           | <30           |
| Pd | <20           | <20           | <20           |
| Ag | <10           | <10           | <10           |
| Cd | <100          | <100          | <100          |
| In | <30           | <30           | <30           |
| Sn | <50           | <50           | <50           |
| Sb | <300          | <300          | <300          |
| Ba | <3            | <3            | <3            |
| Hf | <500          | <500          | <500          |
| Ta | <1000         | <1000         | <1000         |
| W  | 0.1-1%        | 0.1-1%        | 0.1-1%        |
| Ir | Major         | Major         | Major         |
| Pt | <30           | <30           | <30           |
| Au | <10           | <10           | <10           |
| Tl | <30           | <30           | <30           |
| Pb | <30           | <30           | <30           |
| Bi | <30           | <30           | <30           |

TABLE IV  
GPHS LOCK MEMBER COMBINED<sup>a</sup> SHEAR TEST RESULTS

| Test No.          | Load Direction | Ultimate Load, N | Elastic Load, N | Max. Elastic Stress, MPa | Eff. Elastic Shear Mod., MPa/mm        |
|-------------------|----------------|------------------|-----------------|--------------------------|--|
| 1-5Z <sup>c</sup> | XY 0°          | 5208             | 4270            | 14.46                    | 65.4                                   |
| 6-10Z             | XY 45°         | 5476             | 3999            | 13.53                    | 55.1                                   |
| 11-15X            | Z 0°           | 9008             | 3158            | 10.69                    | 46.4 <sup>d</sup><br>32.8 <sup>e</sup> |
| 16-20X            | Z 90°          | 8202             | 5320            | 18.01                    | 61.9                                   |

<sup>a</sup>Five tests averaged in each of four orientations.

<sup>b</sup>The effective modulus is the slope of the elastic portion of the stress-deflection curve.

<sup>c</sup>Letter denotes fiber direction 90° to shear direction.

<sup>d</sup>First elastic region.

<sup>e</sup>Second elastic region.

TABLE V  
DIMENSIONS AND DISPOSITIONS FOR SRL GPHS PELLETS

| SRL Pellets |            |              |            |                | Ir-0.3 Capsules |            |
|-------------|------------|--------------|------------|----------------|-----------------|------------|
| No.         | Diam (in.) | Length (in.) | Weight (g) | Density (% TD) | No.             | Weight (g) |
| GPHS21      | 1.093      | 1.094        | 152.32     | 84.0           | IRG-74          | 51.3       |
| GPHS22      | 1.092      | 1.088        | 151.30     | 84.0           | IRG-76          | 51.8       |
| GPHS25      | 1.087      | 1.085        | 149.29     | 83.9           | IRG-87          | 52.0       |
| GPHS27      | 1.088      | 1.086        | 149.48     | 83.7           | IRG-88          | 52.5       |
| GPHS28      | 1.089      | 1.087        | 149.43     | 82.7           | IRG-89          | 52.4       |
| GPHS29      | 1.089      | 1.085        | 149.39     | 83.7           | IRG-90          | 53.4       |
| GPHS31      | 1.083      | 1.082        | 149.28     | 84.7           |                 |            |

TABLE VI  
LASL RHU PELLETS SUMMARY

|                      |   |
|----------------------|---|
| Feed Material        | <125- $\mu\text{m}$ $^{238}\text{PuO}_2$ granules (LASL lots 38 and 39) seasoned at 1100°C (60 wt%) and 1600°C (40 wt%) |
| Hot Press Parameters | 1530°C for 15 min at 19.5 MPa   |
| Post-Press Sintering | 6 h at 1000°C plus 6 h at 1527°C in Ar-H <sub>2</sub> <sup>16</sup> O   |
| Comments             | 7 lots of 16 pellets each   |

Sintered Dimensions

| <u>Lot</u>    | <u>Diam<br/>(in)</u> | <u>Length<br/>(in)</u> | <u>Weight<br/>(g)</u> | <u>Density<br/>(% TD)</u> |
|---------------|----------------------|------------------------|-----------------------|---------------------------|
| 3             | 0.246                | 0.365                  | 2.664                 | 87.9                      |
| 4             | 0.246                | 0.366                  | 2.665                 | 88.2                      |
| 5             | 0.246                | 0.367                  | 2.667                 | 87.8                      |
| 6             | 0.245                | 0.372                  | 2.665                 | 86.7                      |
| 7             | 0.245                | 0.374                  | 2.662                 | 86.2                      |
| 9             | 0.245                | 0.369                  | 2.664                 | 87.5                      |
| 10            | <u>0.245</u>         | <u>0.369</u>           | <u>2.661</u>          | <u>87.3</u>               |
|               | 0.246<br>$\pm 0.001$ | 0.369<br>$\pm 0.003$   | 2.664<br>$\pm 0.002$  | 87.4<br>$\pm 0.7$         |
| Specification | 0.245<br>$\pm 0.005$ | 0.369<br>$\pm 0.007$   | 2.664<br>$\pm 0.005$  |                           |

TABLE VII  
SPECTROCHEMICAL DATA FOR RHU PELLETS  
(ppm by weight)

| Species | Limit <sup>a</sup> | Sensitivity<br>Limit | Feed Powder    |                  | LWRHU <sup>b</sup><br>Pellets |
|---------|--------------------|----------------------|----------------|------------------|-------------------------------|
|         |                    |                      | SR<br>Analyses | LASL<br>Analyses |                               |
| Al      | 150                | 5                    | 60             | 78               | 147                           |
| B       | 1                  | 1                    | -              | 1                | < <sup>c</sup>                |
| Ca      | 300                | 3                    | 60             | 130              | 44                            |
| Cr      | 250                | 5                    | 97             | 100              | 138                           |
| Cu      | 100                | 1                    | 7              | 15               | <                             |
| Fe      | 800                | 5                    | 262            | 270              | 274                           |
| Mg      | 50                 | 1                    | 15             | 10               | 196                           |
| Mn      | 50                 | 1                    | 8              | 10               | 7                             |
| Mo      | 250                | 20                   | < 50           | 8                | 3                             |
| Na      | 250                | 2                    | 8              | 2                | 3                             |
| Ni      | 150                | 5                    | 45             | 60               | 22                            |
| Pb      | 100                | 5                    | < 10           | 10               | <                             |
| Si      | 200                | 5                    | 78             | 165              | 194                           |
| Sn      | 50                 | 5                    | < 10           | 5                | <                             |
| Zn      | 50                 | 5                    | < 20           | 18               | 14                            |

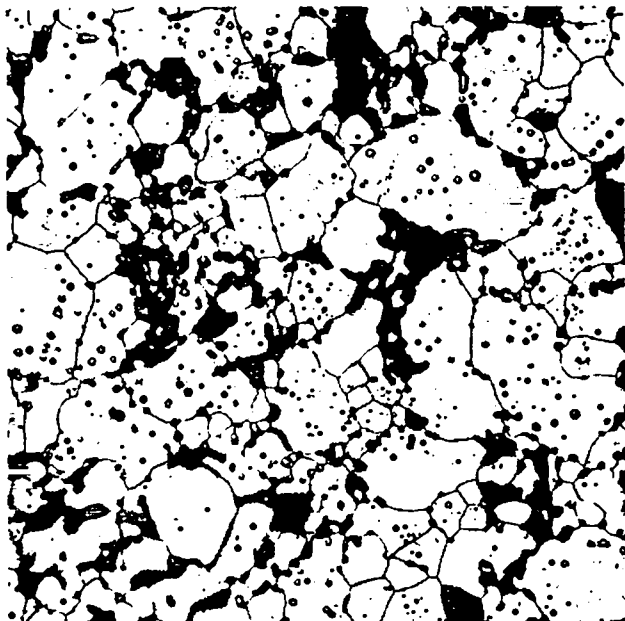
<sup>a</sup>The specification requires that iron and silicon shall not exceed the posted limits. Other cation impurities that exceed the limits shall be reported in the summary data package.

<sup>b</sup>Average for 7 pellet lots.

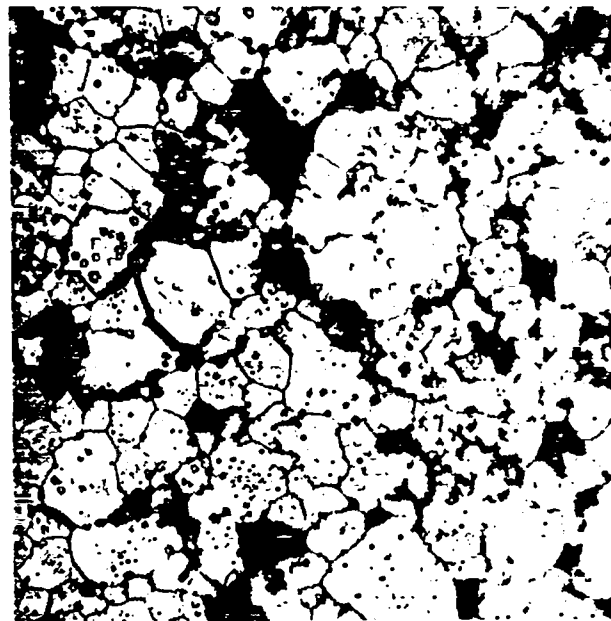
<sup>c</sup>Below sensitivity limit, not detected in these samples.

TABLE VIII  
ISOTOPIC VALUES FOR RHU PELLETS

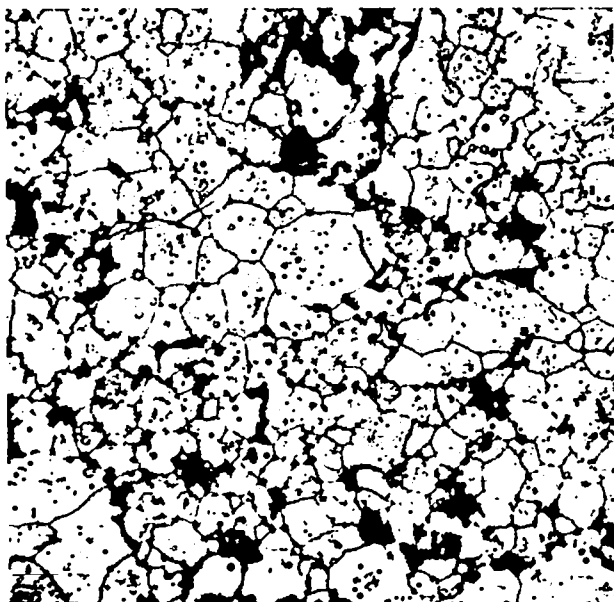
| Isotope           | SR Analyses<br>for Feed |                     | LASL Measurements<br>9/11/80 |       |       |       |       |                   |
|-------------------|-------------------------|---------------------|------------------------------|-------|-------|-------|-------|-------------------|
|                   | Meas.<br>6/27/79        | Decay to<br>9/11/80 | RU 3                         | RU 4  | PU 5  | RU 7  | RU 10 | AV                |
| $^{238}\text{Pu}$ | 83.57                   | 83.47               | 83.41                        | 83.49 | 83.46 | 83.44 | 83.43 | 83.45 $\pm$ 0.03  |
| $^{239}\text{Pu}$ | 13.88                   | 14.00               | 14.04                        | 13.97 | 14.00 | 14.01 | 14.02 | 14.01 $\pm$ 0.03  |
| $^{240}\text{Pu}$ | 1.96                    | 1.98                | 1.98                         | 1.98  | 1.98  | 1.98  | 1.98  | 1.98 $\pm$ 0.00   |
| $^{241}\text{Pu}$ | 0.46                    | 0.44                | 0.440                        | 0.434 | 0.436 | 0.434 | 0.438 | 0.436 $\pm$ 0.003 |
| $^{242}\text{Pu}$ | 0.12                    | 0.12                | 0.130                        | 0.128 | 0.128 | 0.126 | 0.128 | 0.128 $\pm$ 0.002 |



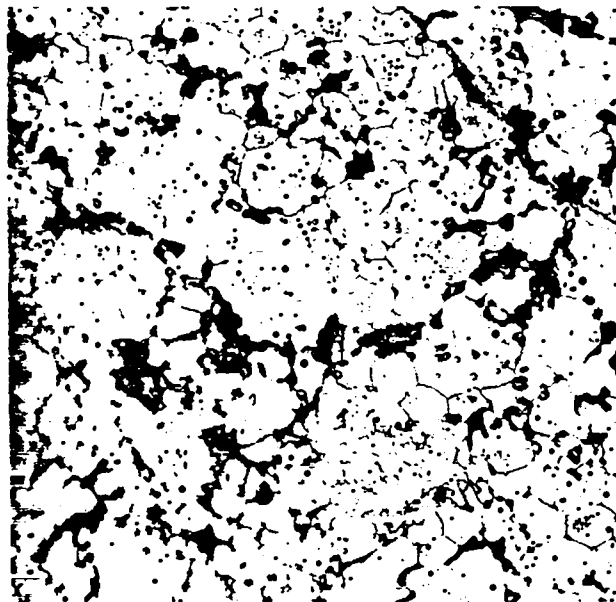
(a)



(b)



(c)



(d)

Fig. 1.  
The microstructures of the impacted DVT fuel pellets were quite similar. a) IRG-87 (GPHS-25); b) IRG-88 (GPHS-27); c) IRG-89 (GPHS-28); and d) IRG-90 (GPHS-29). 250X.

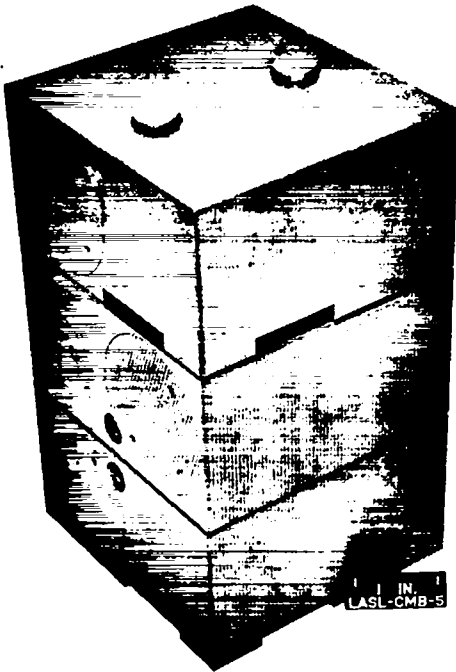


Fig. 2.  
The module's position in the heat source stack is maintained by the lock members visible on top of the stack.

## -SHEAR TEST FIXTURE- LOCK MEMBER SHEAR TEST

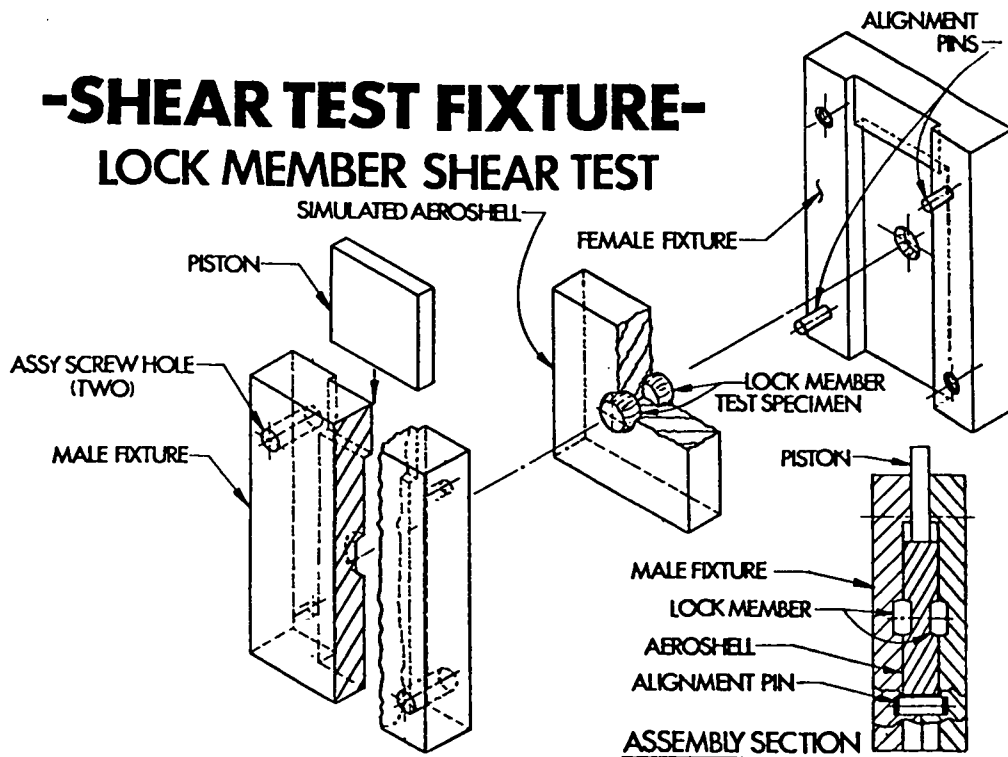


Fig. 3.  
The lock-member shear tests were carried out using a shear fixture that simultaneously loaded two lock members.



Fig. 4.  
The parts of the shear-test fixture are all visible in this photograph.

Z BUNDLE ORIENTATION RELATIVE TO SHEAR TEST DIRECTION

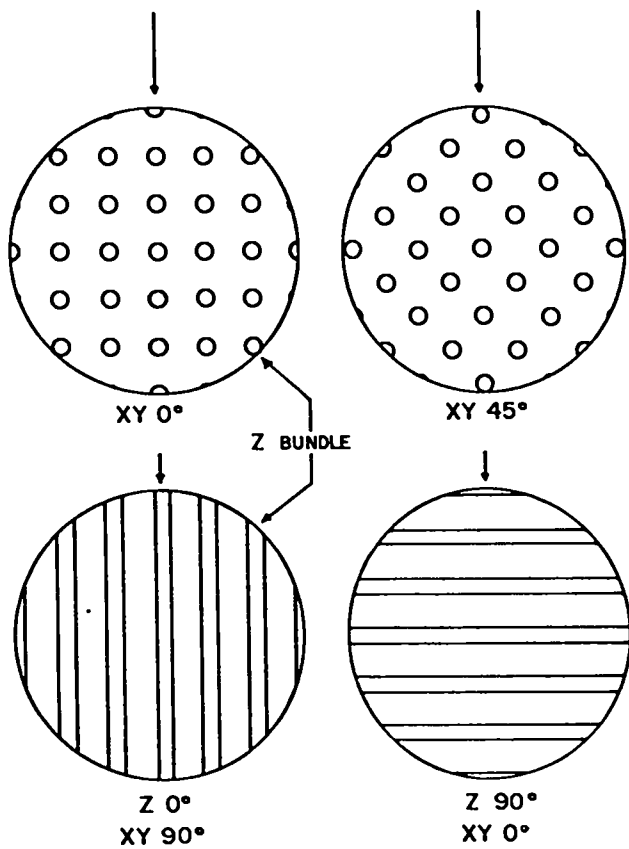
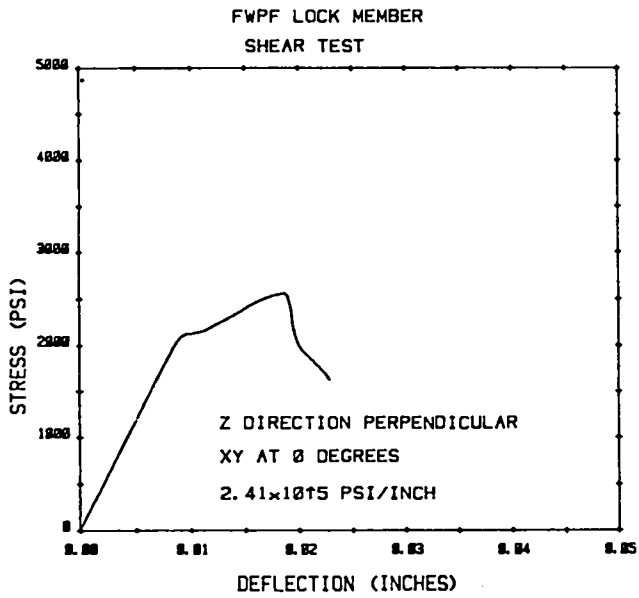
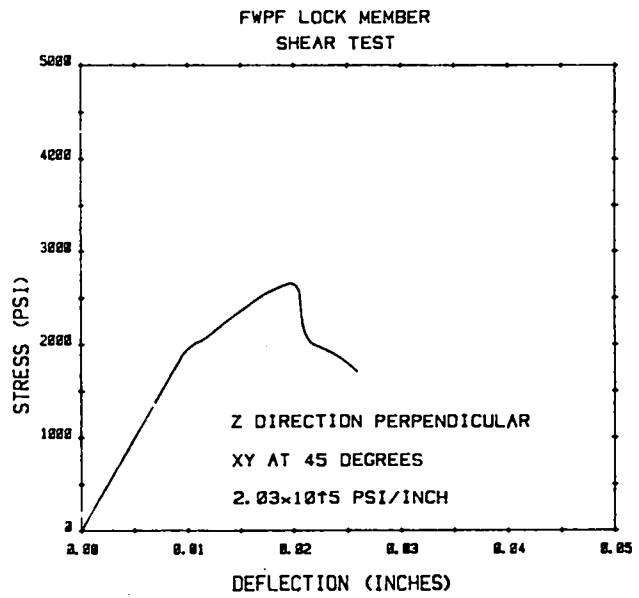


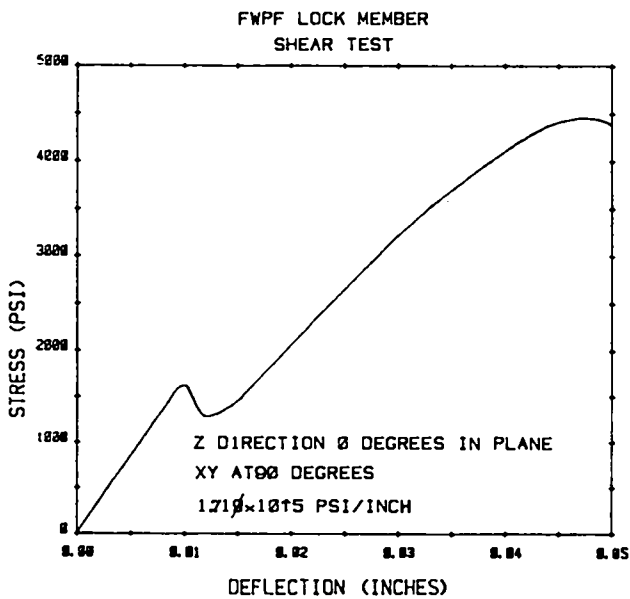
Fig. 5.  
Four characteristic orientations for the FWP structure were tested in shear (arrows).



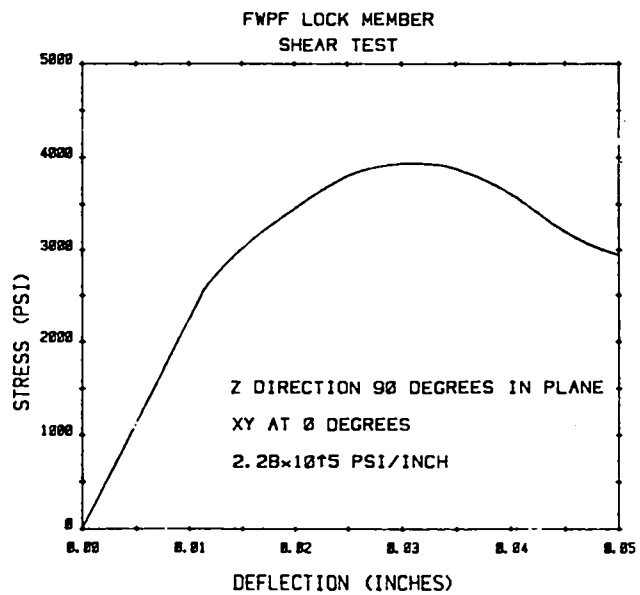
(a)



(b)



(c)



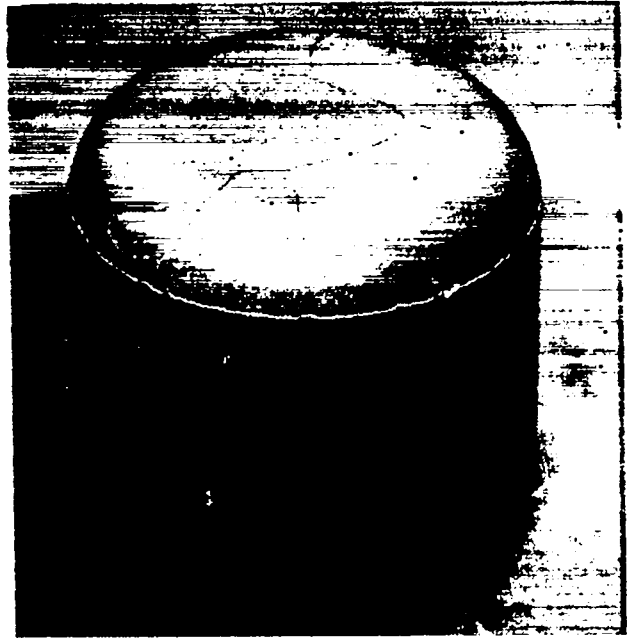
(d)

Fig. 6.

The shapes shear stress vs deflection curves for FWPf varied with the orientation of the microstructure of the composite. a) Z perpendicular, XY at 0°; b) Z perpendicular, XY at 45°; c) Z parallel and 0°; and d) Z parallel and 90°.



(a)

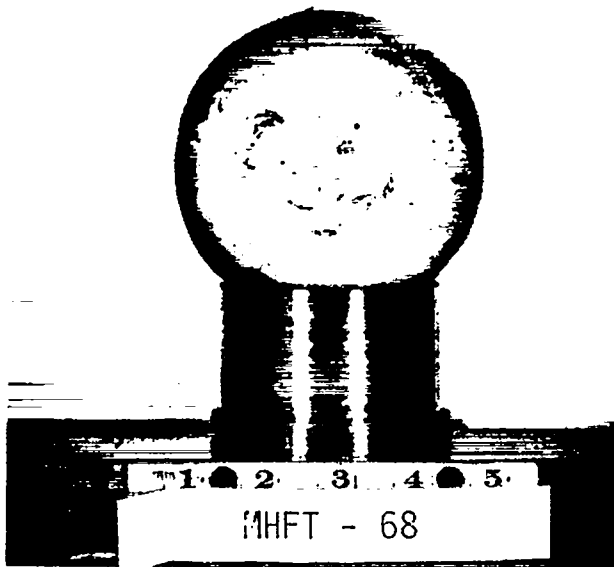


(b)

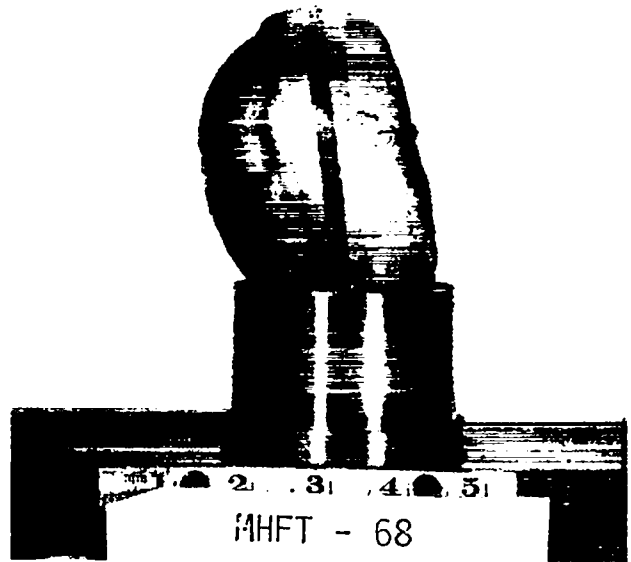


(c)

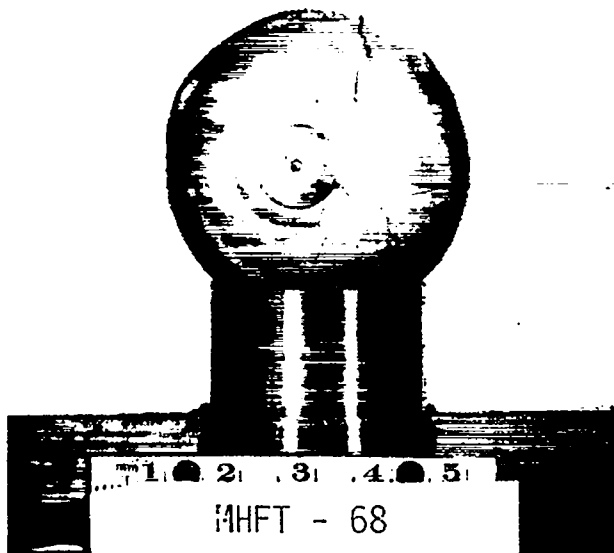
Fig. 7.  
The GPHS fuel pellets received from Savannah River Laboratory all contained surface cracks. a) GPHS-28; b) GPHS-29; and c) GPHS-31.



(a)



(b)



(c)

Fig. 8.  
Photographs of the impacted sample from  
MHFT-68. a) Impact face, b) profile  
view, and c) back side.  $\times 1X$ .

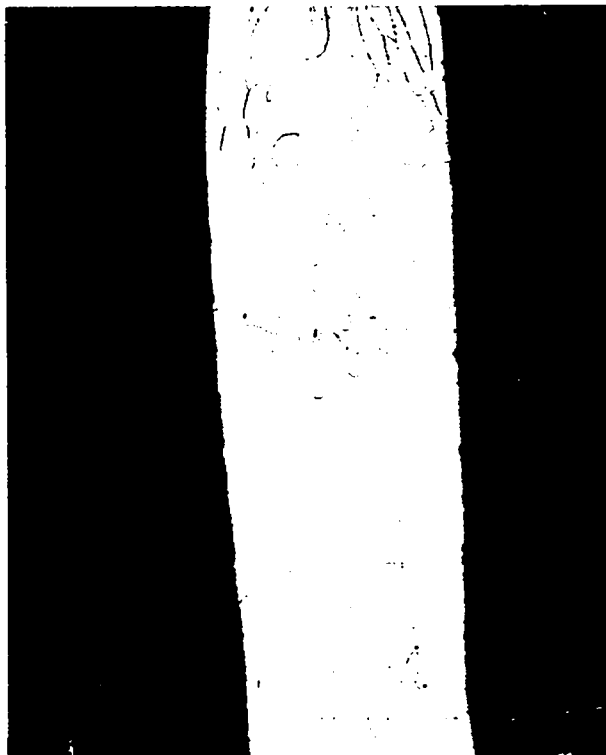
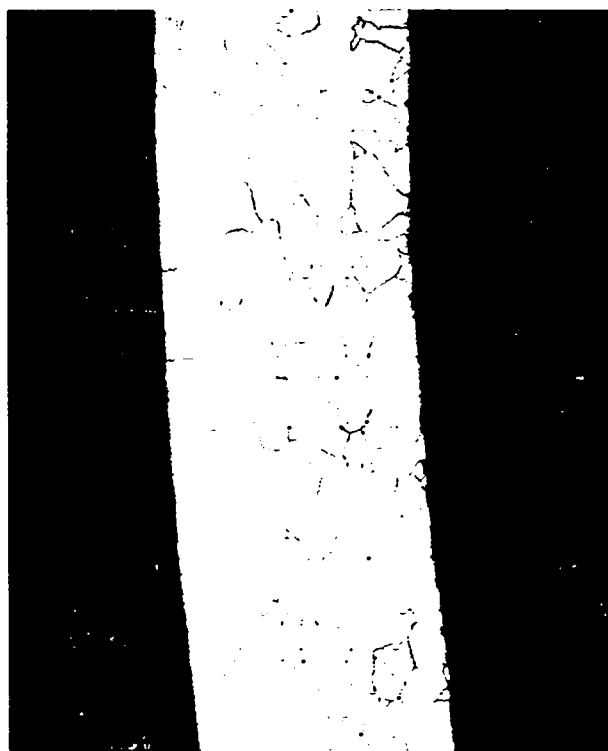
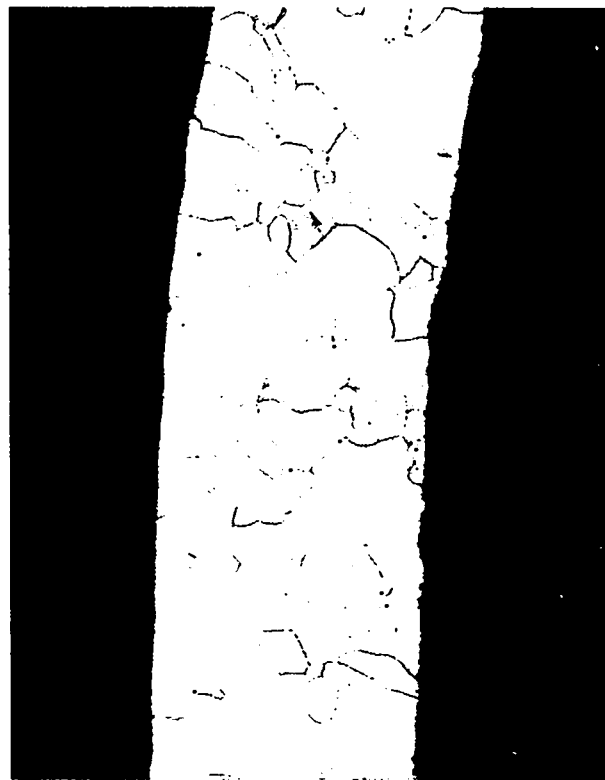


Fig. 9.  
Microstructure of the equatorial weld  
of the iridium shell of MHFT-68. 40X



(a)



(b)

Fig. 10.  
Microstructures of one hemishell from the iridium shell of MHFT-68. 50X.

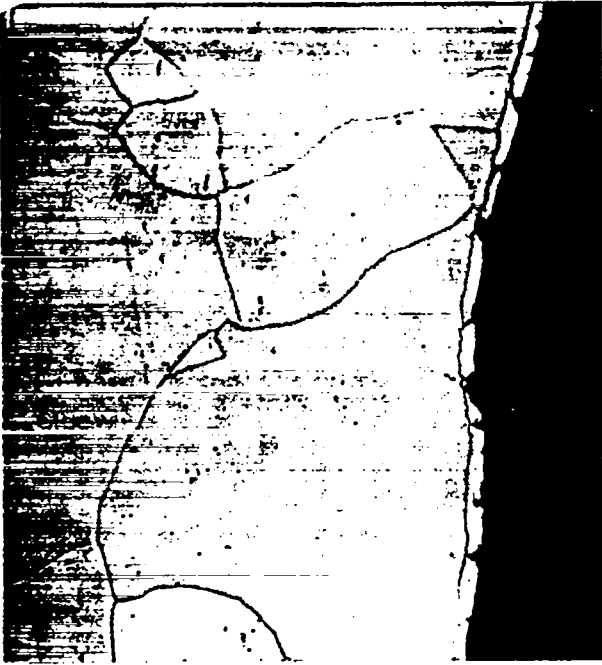


Fig. 11.  
Photomicrograph illustrating the occurrence of flat grains of iridium on the inside surface of the iridium shell of MHFT-68. 250X.

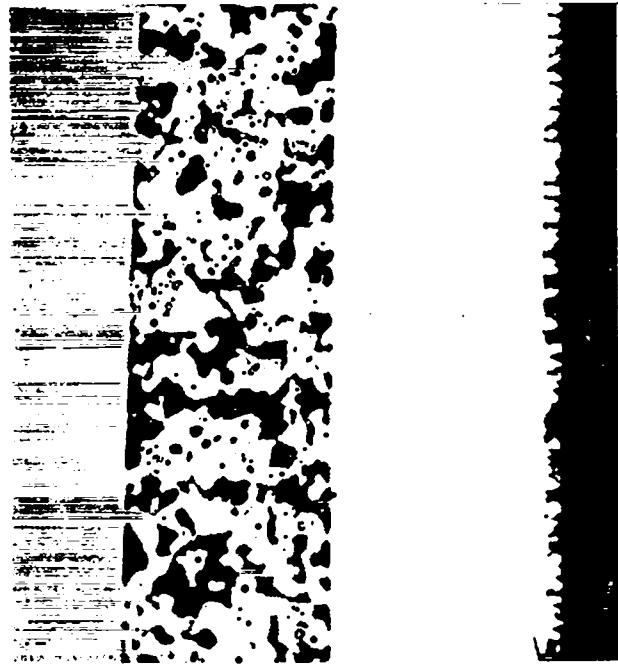
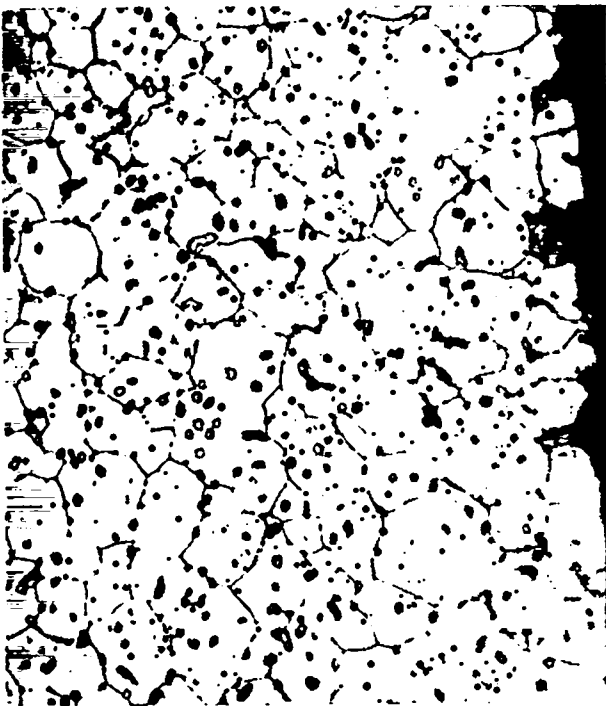
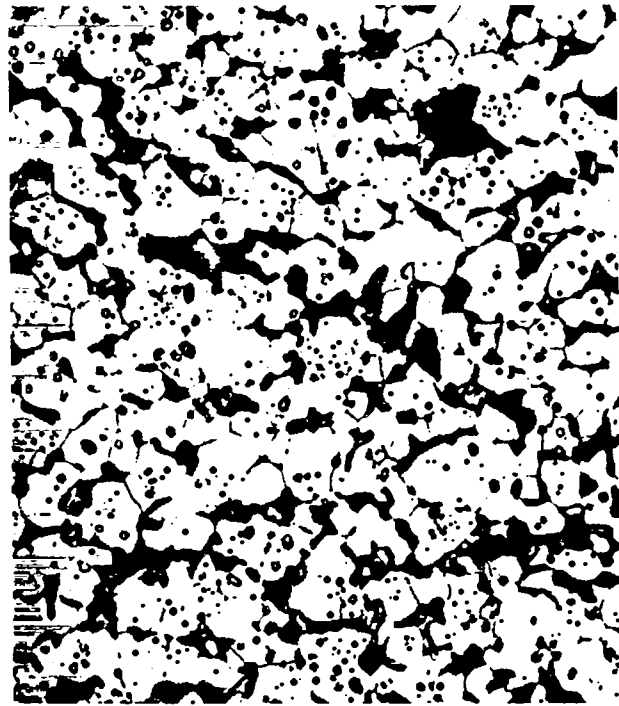


Fig. 12.  
Photomicrograph illustrating a small amount of iridium transport in the interior of the iridium shell of MHFT-68. 250X.



(a)



(b)

Fig. 13.  
Microstructures of the plutonia sphere from MHFT-68. a) Area near the impact face surface, and b) area removed from the impact face surface. 250X.

## ADDITIONAL DISTRIBUTION

B. J. Rock, Dept. of Energy/ANSP, Washington, DC  
G. L. Bennett, Dept. of Energy/ANSP, Washington, DC  
J. J. Lombardo, Dept. of Energy/ANSP, Washington, DC  
P. B. Morrow, Dept. of Energy/ANSP, Washington, DC  
C. O. Tarr, Dept. of Energy/ANSP, Washington, DC  
R. Brouns, Dept. of Energy/ANSP, Washington, DC  
J. Griffio, Dept. of Energy/ANSP, Washington, DC  
J. L. Liverman, Dept. of Energy/ANSP, Washington, DC  
R. Ferguson, Dept. of Energy/ET, Washington, DC  
D. K. Stevens, Dept. of Energy/BES, Washington, DC  
H. E. Roser, Dept. of Energy/ALO, Albuquerque, NM  
W. McMullins, Dept. of Energy/ALO, Albuquerque, NM  
D. L. Plymale, Dept. of Energy/ALO, Albuquerque, NM  
H. N. Hill, Dept. of Energy/DOA, Miamisburg, OH  
M. J. Sires, Dept. of Energy/SRO, Aiken, SC  
R. J. Hart, Dept. of Energy/ORO, Oak Ridge, TN  
W. L. Von Flue, Dept. of Energy, SFOO, Oakland, CA  
T. B. Kerr, NASA, Washington, DC  
R. A. Ivanoff, NASA/JPL, Pasadena, CA  
G. Stapfer, NASA/JPL, Pasadena, CA  
R. Campbell, NASA/JPL, Pasadena, CA  
AFISC/SNS, Attn: Col. J. A. Richardson, KAFB, Albuquerque, NM  
AFWL/NTYVS, Attn: Capt. J. D. Martens, KAFB, Albuquerque, NM  
HQ Space Div./YLVS: Attn: Lt. Col. Needham, Los Angeles, CA  
R. L. Folger, SRL, Aiken, SC  
R. H. Tait, SRL, Aiken, SC  
J. B. Mellen, SRP, Aiken, SC  
G. W. Wilds, SRP, Aiken, SC  
R. A. Brownback, SRP, Aiken, SC  
J. R. McClain, MRC, Miamisburg, OH  
W. T. Cave, MRC, Miamisburg, OH  
W. Amos, MRC, Miamisburg, OH  
E. W. Johnson, MRC, Miamisburg, OH  
H. Postma, ORNL, Oak Ridge, TN  
R. Cooper, ORNL, Oak Ridge, TN  
H. Inouye, ORNL, Oak Ridge, TN  
E. Foster, BCL, Columbus, OH  
I. Grinberg, BCL, Columbus, OH  
C. Alexander, BCL, Columbus, OH  
E. E. Rice, BCL, Columbus, OH  
J. Hagan, APL, Baltimore, MD  
R. W. Englehart, NUS Corp., Rockville, MD  
H. H. Van Tuyl, PNL, Richland, WA  
A. Schock, Fairchild-Hiller Ind., Germantown, MD  
C. W. Whitmore, GE, Philadelphia, PA  
R. Hemler, GE, Philadelphia, PA  
V. Haley, GE, Philadelphia, PA  
E. C. Krueger, Sundstrand, Rockford, IL  
F. Schumann, TES, Timonium, MD  
J. Boretz, TRW, Redondo Beach, CA  
R. Hartman, GE, Philadelphia, PA

W. Mecham, ANL, Argonne, IL  
G. A. Cowan, Los Alamos, NM  
R. D. Baker, Los Alamos, NM  
R. N. R. Mulford, Los Alamos, NM  
W. F. Miller, Los Alamos, NM  
R. J. Pryor, Los Alamos, NM  
G. R. Waterbury, Los Alamos, NM  
R. Behrens, Los Alamos, NM  
S. E. Bronisz, Los Alamos, NM  
R. A. Kent, Los Alamos, NM  
W. Stark, Los Alamos, NM  
R. W. Zocher, Los Alamos, NM  
J. A. Pattillo, Los Alamos, NM

Printed in the United States of America  
 Available from  
 National Technical Information Service  
 US Department of Commerce  
 5285 Port Royal Road  
 Springfield, VA 22161  
 Microfiche \$3.50 (A01)

| Page Range | Domestic Price | NTIS Price Code | Page Range | Domestic Price | NTIS Price Code | Page Range | Domestic Price | NTIS Price Code | Page Range | Domestic Price | NTIS Price Code |
|------------|----------------|-----------------|------------|----------------|-----------------|------------|----------------|-----------------|------------|----------------|-----------------|
| 001-025    | \$ 5.00        | A02             | 151-175    | \$11.00        | A08             | 301-325    | \$17.00        | A14             | 451-475    | \$23.00        | A20             |
| 026-050    | 6.00           | A03             | 176-200    | 12.00          | A09             | 326-350    | 18.00          | A15             | 476-500    | 24.00          | A21             |
| 051-075    | 7.00           | A04             | 201-225    | 13.00          | A10             | 351-375    | 19.00          | A16             | 501-525    | 25.00          | A22             |
| 076-100    | 8.00           | A05             | 226-250    | 14.00          | A11             | 376-400    | 20.00          | A17             | 526-550    | 26.00          | A23             |
| 101-125    | 9.00           | A06             | 251-275    | 15.00          | A12             | 401-425    | 21.00          | A18             | 551-575    | 27.00          | A24             |
| 126-150    | 10.00          | A07             | 276-300    | 16.00          | A13             | 426-450    | 22.00          | A19             | 576-600    | 28.00          | A25             |
|            |                |                 |            |                |                 |            |                |                 | 601-up     | †              | A99             |

†Add \$1.00 for each additional 25-page increment or portion thereof from 601 pages up.